Inorg. Chem. **2009**, *48*, 3800−3807

Ligand-Dependent Ultrasonic-Assistant Self-Assemblies and Photophysical Properties of Lanthanide Nicotinic/Isonicotinic Complexes

Wentong Chen[†,‡] and Shunichi Fukuzumi*[,†]

Department of Material and Life Science, Graduate School of Engineering, Osaka University, Suita, SORST, Japan Science Technology Agency, Osaka 565-0871, Japan, and School of Chemistry and Chemical Engineering, Jinggangshan University, Ji'an, Jiangxi 343009, China

Received January 9, 2009

Two structural series, including two isomorphous homodinuclear complexes $Ln_2(H_2O)_4(C_6NO_2H_4)_6$ (Ln = Tb (**1**) and Er (**2**)) and four isostructural one-dimensional (1-D) chain-like assemblies $[Ln(H_2O)_4(C_6NO_2H_4)_2]_n \cdot n$Cl (Ln = Sm (**3**), Eu (**4**), Tb (**5**), and Dy (**6**)), have been rationally prepared through a facile ultrasonic synthesis and have been characterized by X-ray diffraction and photophysical measurements. Both complexes, **1** and **2**, feature a homodinuclear structure, based on two 8-fold coordination lanthanide atoms bridged by four nicotinic acid ligands. Complexes **3**−**6** are characterized by a 1-D polycationic chain-like structure, containing eight-coordinated lanthanide ions and bridging isonicotinic acid ligands. The 1-D polycationic chains and the isolated chloride anions are interconnected via hydrogen bonds and π-π interactions to form a three-dimensional supramolecular network. The effect of nicotinic/isonicotinic acid ligands on the structures and the photoluminescence properties, as well as the relationship between the photoluminescence properties and the structures, was investigated based on IR, UV−vis absorption spectra, low temperature phosphorescent spectra, excitation, and emission spectra. The fluorescence quantum yields of complexes **1** and **2** were determined to be 44% and 21%, respectively.

Introduction

Lanthanide complexes have attracted increasing interest because of their photoluminescent properties and, in recent years, much research has been carried out on lanthanide complexes with conjugated organic ligands because they display properties desirable for potential applications in luminescent materials or luminescence probes and so on.[1−19] Lanthanides possess f-f electronic orbitals, and if transition of the lanthanide ions took place, they would show strong emission bands. However, lanthanide ions usually have low absorption coefficients that make the f-f electronic transition difficult and results in weak or non-existent emission bands.

* To whom correspondence should be addressed. E-mail: fukuzumi@chem.eng.osaka-u.ac.jp. Fax: (+81) 6-6879-7370.
† Osaka University.
‡ Jinggangshan University.

(1) (a) Bünzli, J.-C. G. Rare Earth Luminescent Centers in Organic and Biochemical Compounds. In *Spectroscopic Properties of Rare Earths in Optical Materials*; Liu, G. K., Jacquier, B., Eds.; Springer-Verlag: Berlin, Germany, 2005; Vol. *83*, Chapter 11. (b) Cotton, S. *Lanthanide and actinide chemistry*; John Wiley & Sons: New York, 2006. (c) Jones, C. *D-And F-Block Chemistry*; Royal Society of Chemistry: London, 2000.
(2) (a) Bünzli, J.-C. G. *Acc. Chem. Res.* **2006**, *39*, 53. (b) Bünzli, J.-C. G.; Piguet, C. *Chem. Soc. Rev.* **2005**, *34*, 1048. (c) Bünzli, J.-C. G.; Piguet, C. *Chem. Rev.* **2002**, *102*, 1897. (d) Edelmann, F. T. *Coord. Chem. Rev.* **2009**, *253*, 343. (e) Que, E. L.; Domaille, D. W.; Chang, C. J. *Chem. Rev.* **2008**, *108*, 1517. (f) Santos, C. M. G.; Harte, A. J.; Quinn, S. J.; Gunnlaugsson, T. *Coord. Chem. Rev.* **2008**, *252*, 2512. (g) Wong, W.-K.; Zhu, X.; Wong, W.-Y. *Coord. Chem. Rev.* **2007**, *251*, 2386.
(3) de Bettencourt-Dias, A.; Viswanathan, S.; Rollett, A. *J. Am. Chem. Soc.* **2007**, *129*, 15436.
(4) de Bettencourt-Dias, A. *Inorg. Chem.* **2005**, *44*, 2734.
(5) de Bettencourt-Dias, A. *Curr. Org. Chem.* **2007**, *11*, 1460.
(6) de Bettencourt-Dias, A. *Dalton Trans.* **2007**, *22*, 2229.
(7) Petoud, S.; Muller, G.; Moore, E. G.; Xu, J.; Sokolnicki, J.; Riehl, J. P.; Le, U. N.; Cohen, S. M.; Raymond, K. N. *J. Am. Chem. Soc.* **2007**, *129*, 77.
(8) Petoud, S.; Cohen, S. M.; Bünzli, J.-C. G.; Raymond, K. N. *J. Am. Chem. Soc.* **2003**, *125*, 13324.
(9) Weibel, N.; Charbonnère, L.; Guardigli, M.; Roda, A.; Ziessel, R. *J. Am. Chem. Soc.* **2004**, *126*, 4888.
(10) Law, G.-L.; Wong, K.-L.; Man, C. W.-Y.; Wong, W.-T.; Tsao, S.-W.; Lam, M. H.-W.; Lam, P. K.-S. *J. Am. Chem. Soc.* **2008**, *130*, 3714.
(11) Zheng, X.-L.; Liu, Y.; Pan, M.; Lu, X.-Q.; Zhang, J.-Y.; Zhao, C.-Y.; Tong, Y.-X.; Su, C.-Y. *Angew. Chem., Int. Ed.* **2007**, *46*, 7399.
(12) Cummins, C. M.; Koivunen, M. E.; Stephanian, A.; Gee, S. J.; Hammock, B. D.; Kennedy, I. M. *Biosens. Bioelectron.* **2006**, *21*, 1077.
(13) Remya, P. N.; Biju, S.; Reddy, M. L. P.; Cowley, A. H.; Findlater, M. *Inorg. Chem.* **2008**, *47*, 7396.
(14) Xin, H.; Li, F. Y.; Shi, M.; Bian, Z. Q.; Huang, C. H. *J. Am. Chem. Soc.* **2003**, *125*, 7166.
(15) Seitz, M.; Moore, E. G.; Ingram, A. J.; Muller, G.; Raymond, K. N. *J. Am. Chem. Soc.* **2007**, *129*, 15468.

10.1021/ic9000279 CCC: $40.75
Published on Web 03/18/2009

Therefore efforts have been made to increase the absorption coefficients and hence obtain intense emissions of the lanthanide ions. This can be accomplished through careful selection of organic ligands with conjugated motifs, such as aromatic carboxylic acids, β-diketones and heterocyclic derivatives because these organic ligands can absorb ultraviolet light and transfer the absorbed energy to the central lanthanide ions effectively (so-called antenna effect).[20−23]

The "antenna" ligand's intersystem crossing quantum yield, the antenna-lanthanide ion distance, and the energy match (exactly the energy difference) between the triplet state energy of an "antenna" ligand and the resonant energy level of a lanthanide ion are the main factors in attaining efficient emission of a lanthanide ion.[24] Among the aforementioned factors, the energy match for the intramolecular energy migration efficiency from the organic ligands to the central Ln^{3+} ions plays the most important role. An efficient emission of a lanthanide ion is possible only when a good energy match is attained. This is known as the energy match mechanism.[25] By virtue of the energy transfer and the energy match mechanism, it is possible to predict the photoluminescent properties of a lanthanide complex. When aromatic carboxylic acids are employed as the organic ligands, lanthanide ions exhibit higher luminescent stability for practical applications than those possessing other organic ligands.[26−28] Among aromatic carboxylic acids, nicotinic/isonicotinic acids have a conjugated structural motif, and they are quite interesting synthons in constructing extended structures because they are unsymmetrical divergent ligands. They can link two or three metal centers by coordinating to a metal ion with the nitrogen atom and to other metal ion(s) with one or two carboxylato oxygen atoms (Scheme 1). Although a number of lanthanide-nicotinic/isonicotinic acid complexes have so far been documented,[29−38] the investigations on the relationship between the crystal structures and the photoluminescent properties have scarcely been performed.

Scheme 1. Various Coordination Modes of Nicotinic (Upper) and Isonicotinic (Bottom) with Metal Ions (M = Metal Ion)

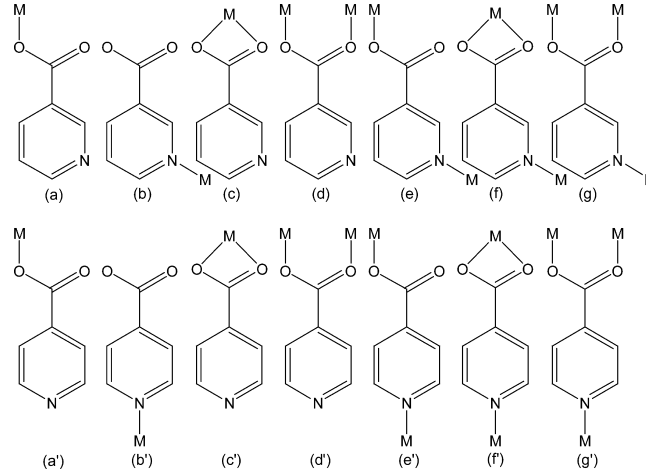

To gain new insights into the relationship between the crystal structures and the photoluminescent properties, and the effects of ligands on the photoluminescent properties and the crystal structures, we chose nicotinic/isonicotinic acid as organic ligands to prepare new lanthanide complexes and investigate their crystal structures and photoluminescent properties. We report herein the synthesis and X-ray crystal structures of a series of lanthanide complexes: homodinuclear $Tb_2(H_2O)_4(C_6NO_2H_4)_6$ (**1**) and $Er_2(H_2O)_4(C_6NO_2H_4)_6$ (**2**) and four isostructural one-dimensional (1-D) polycationic chain-like assemblies $[Ln(H_2O)_4(C_6NO_2H_4)_2]_n \cdot n$Cl (Ln = Sm (**3**), Eu (**4**), Tb (**5**), and Dy (**6**)). These lanthanide complexes were prepared by an ultrasonic reaction method,[39−41] which is different from traditional solution methods or solvothermal reactions. Ultrasonic irradiation has several advantages compared with conventional reaction methods in the syntheses of organic or inorganic materials. Easy operation and mild reaction conditions are two prominent features of ultrasonic irradiation reactions as compared with conventional reaction methods. Moreover, ultrasonic irradiation is also useful in enhancing the reaction rates and shortening the reaction time in many systems.

The series of lanthanide complexes newly synthesized and structurally characterized in this study provide an excellent opportunity to clarify the relationship between the photoluminescence properties and the structures of **1**−**6** by using IR, UV−vis absorption spectra, low temperature phosphorescent spectra, excitation and emission spectra.

(16) Ai, K. L.; Zhang, B. H.; Lu, L. H. *Angew. Chem., Int. Ed.* **2009**, *48*, 304.
(17) Jeong, N. C.; Lee, J. S.; Tae, E. L.; Lee, Y. J.; Yoon, K. B. *Angew. Chem., Int. Ed.* **2008**, *47*, 10128.
(18) Mizukami, S; Tonai, K; Kaneko, M; Kikuchi, K. *J. Am. Chem. Soc.* **2008**, *130*, 14376.
(19) Keizers, P. H. J.; Saragliadis, A.; Hiruma, Y.; Overhand, M.; Ubbink, M. *J. Am. Chem. Soc.* **2008**, *130*, 14802.
(20) Samuel, A. P. S.; Moore, E. G.; Melchior, M.; Xu, J.; Raymond, K. N. *Inorg. Chem.* **2008**, *47*, 7535.
(21) Picot, A.; Malvolti, F.; Le Guennic, B.; Baldeck, P. L.; Williams, J. A. G.; Andraud, C.; Maury, O. *Inorg. Chem.* **2007**, *46*, 2659.
(22) Shen, L.; Shi, M.; Li, F.; Zhang, D.; Li, X.; Shi, E.; Yi, T.; Du, Y.; Huang, C. *Inorg. Chem.* **2006**, *45*, 6188.
(23) Yan, B.; Zhou, B. *J. Photochem. Photobiol. A Chem.* **2005**, *171*, 181.
(24) Latva, M.; Takalo, H.; Mukkala, V.-M.; Matachescu, C.; Rodriguez-Ubis, J. C.; Kankare, J. *J. Lumin.* **1997**, *75*, 149.
(25) Yan, B.; Xu, B. *J. Fluoresc.* **2005**, *15*, 619.
(26) Yan, B.; Zhu, H. X. *J. Fluoresc.* **2007**, *17*, 331.
(27) Charbonnère, L. J.; Weibel, N.; Retailleau, P.; Ziessel, R. *Chem.—Eur. J.* **2007**, *13*, 346.
(28) Jin, L. P.; Lu, S. X.; Lu, S. Z. *Polyhedron* **1996**, *15*, 4069.
(29) Guillou, O.; Daiguebonne, C. *Handbook on the Physics and Chemistry of Rare Earths*; Elsevier: Amsterdam, 2004; Vol. *34*, Chapter 221, p 359.
(30) Cheng, J.-W.; Zheng, S.-T.; Yang, G.-Y. *Inorg. Chem.* **2008**, *47*, 4930.
(31) Jia, G.; Law, G.-L.; Wong, K.-L.; Tanner, P. A.; Wong, W.-T. *Inorg. Chem.* **2008**, *47*, 9431.
(32) Li, Y.-W.; Wang, Y.-H.; Li, Y.-G.; Wang, W.-B. *J. Solid State Chem.* **2008**, *181*, 1485.
(33) Mou, J.-X.; Zeng, R.-H.; Qiu, Y.-C.; Zhang, W.-G.; Deng, H.; Zeller, M. *Inorg. Chem. Commun.* **2008**, *11*, 1347.
(34) Cheng, J.-W.; Zheng, S.-T.; Yang, G.-Y. *Dalton Trans.* **2007**, *36*, 4059.
(35) Ma, L.; Evans, O. R.; Foxman, B. M.; Lin, W. *Inorg. Chem.* **1999**, *38*, 5837.
(36) Zhang, D.-J.; Song, T.-Y.; Wang, L.; Shi, J.; Xu, J.-N.; Wang, Y.; Ma, K.-R.; Yin, W.-R.; Zhang, L.-R.; Fan, Y. *Inorg. Chim. Acta* **2009**, *362*, 299.
(37) Liu, Z.-H.; Qiu, Y.-C.; Li, Y.-H.; Deng, H.; Zeller, M. *Polyhedron* **2008**, *27*, 3493.
(38) Zhou, Y.-X.; Shen, X.-Q.; Zhang, H.-Y.; Du, C.-X.; Wu, B.-L.; Hou, H.-W. *J. Coord. Chem.* **2008**, *61*, 3981.
(39) Richards, W. T.; Loomis, A. L. *J. Am. Chem. Soc.* **1927**, *49*, 3086.
(40) Grinstaff, M. W.; Cichowlas, A. A.; Choe, S. B.; Suslick, K. S. *Ultrasonics* **1992**, *30*, 168.
(41) Misik, V.; Miyoshi, N.; Riesz, P. *J. Phys. Chem.* **1995**, *99*, 3605.

Experimental Section

Measurements. Elemental analyses of carbon, hydrogen, and nitrogen were carried out with an Elementar Vario EL III microanalyser. The infrared spectra were recorded on a Thermo Nicolet NEXUS 870 FT-IR spectrophotometer over the frequency range 4000−400 cm^{-1} using the KBr pellet technique. The UV−vis absorption spectroscopies were recorded at room temperature on a computer-controlled Hewlett-Packard 89090A UV−vis spectrometer with the wavelength range of 190−1100 nm. The phosphorescence spectra and the solid-state fluorescent studies were conducted on a Shimadzu RF-530XPC fluorescence spectroscopy instrument under 77 K and room temperature, respectively. Measurement of emission quantum yields of powdered samples, which were carried out on a Hamamatsu C9920-0X(PMA-12) U6039-05 fluorescence spectrofluorometer with an integrating sphere adapted to a right angle configuration at room temperature, involved determination of the diffuse reflectance spectra of the samples, and the measured results were corrected for the detector response as a function of wavelength.

Syntheses. All reactants of A.R. grade were obtained commercially and used without further purification.

$Tb_2(H_2O)_4(C_6NO_2H_4)_6$ (1). $TbCl_3 \cdot 6H_2O$ (1 mmol, 373.4 mg) and nicotinic acid (2 mmol, 246.2 mg) were dissolved by 50 mL of distilled water, then ultrasonicated for 3 h and filtered. The filtrate was left to stand at room temperature for 3 weeks, and colorless crystals suitable for X-ray analysis were obtained. Yield: 24% (based on terbium). Anal. Calcd for $C_{36}H_{32}N_6O_{16}Tb_2$: C, 38.49; H, 2.85; N, 7.48. Found: C, 38.23; H, 2.86; N, 7.41. Fourier transform IR (KBr, cm^{-1}): 3291(vs), 2362(m), 1926(w), 1660(vs), 1644(vs), 1591(vs), 1549(vs), 1527(vs), 1410(vs), 1198(s), 1166(m), 1092(m), 1027(vs), 965(w), 943(s), 864(vs), 757(vs) and 699(s).

$Er_2(H_2O)_4(C_6NO_2H_4)_6$ (2). This complex was prepared by the procedure described for **1** using $ErCl_3$ (1 mmol, 273.6 mg) instead of $TbCl_3 \cdot 6H_2O$. Yield: 27% (based on erbium). Anal. Calcd for $C_{36}H_{32}Er_2N_6O_{16}$: C, 37.92; H, 2.81; N, 7.37. Found: C, 36.87; H, 2.90; N, 7.10. Fourier transform IR (KBr, cm^{-1}): 3275(vs), 2361(m), 1926(w), 1661(vs), 1639(vs), 1592(vs), 1549(vs), 1411(vs), 1193(vs), 1166(m), 1097(s), 1028(vs), 975(m), 868(vs), 762(vs), 694(m) and 629(w).

$[Sm(H_2O)_4(C_6NO_2H_4)_2]_n \cdot n$Cl (3). Complex **3** was prepared by the procedure described for **1** using $SmCl_3 \cdot 6H_2O$ (1 mmol, 364.8 mg) and isonicotinic acid (2 mmol, 246.2 mg) instead of $TbCl_3 \cdot 6H_2O$ and nicotinic acid. Yield: 20% (based on samarium). Anal. Calcd for $C_{12}H_{16}ClN_2O_8Sm$: C, 28.69; H, 3.19; N, 5.58. Found: C, 28.64; H, 3.12; N, 5.62. Fourier transform IR (KBr, cm^{-1}): 3259(vs), 2823(vs), 2245(s), 1969(w), 1644(vs), 1593(vs), 1549(vs), 1501(vs), 1413(vs), 1230(s), 1161(m), 1060(vs), 1012(vs), 867(m), 852(s), 773(s), 715(m), and 683(m).

$[Eu(H_2O)_4(C_6NO_2H_4)_2]_n \cdot n$Cl (4). This complex was prepared by the procedure described for **1** using $EuCl_3 \cdot 6H_2O$ (1 mmol, 366.4 mg) and isonicotinic acid (2 mmol, 246.2 mg) instead of $TbCl_3 \cdot 6H_2O$ and nicotinic acid. Yield: 18% (based on europium). Anal. Calcd for $C_{12}H_{16}ClEuN_2O_8$: C, 28.59; H, 3.18; N, 5.56. Found: C, 28.51; H, 3.10; N, 5.58. Fourier transform IR (KBr, cm^{-1}): 3397 (vs), 3240(vs), 3040(w), 2359(w), 1957(w), 1590(vs), 1545(vs), 1495(m), 1416(vs), 1227(m), 1060(m), 1004(m), 864(m), 775(s), 713(m), and 680(m).

$[Tb(H_2O)_4(C_6NO_2H_4)_2]_n \cdot n$Cl (5). Complex **5** was prepared by the procedure described for **1** using isonicotinic acid (2 mmol, 246.2 mg) instead of nicotinic acid. Yield: 23% (based on terbium). Anal. Calcd for $C_{12}H_{16}ClN_2O_8Tb$: C, 28.20; H, 3.13; N, 5.48. Found: C, 28.39; H, 3.00; N, 5.54. Fourier transform IR (KBr, cm^{-1}): 3435(vs), 3036(w), 2362(w), 1968(w), 1592(vs), 1549(vs), 1495(m), 1413(vs), 1230(m), 1060(s), 1012(s), 852(m), 768(s), 715(m), and 683(s).

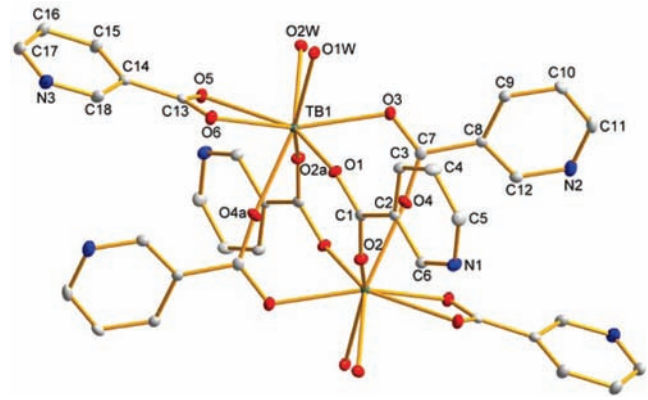

Figure 1. ORTEP drawing of **1** with 30% thermal ellipsoids. Hydrogen atoms were omitted for clarity. Symmetry codes: a. $-2-x, 1-y, -1-z$.

$[Dy(H_2O)_4(C_6NO_2H_4)_2]_n \cdot n$Cl (6). This complex was prepared by the procedure described for **1** using $DyCl_3 \cdot 6H_2O$ (1 mmol, 377.0 mg) and isonicotinic acid (2 mmol, 246.2 mg) instead of $TbCl_3 \cdot 6H_2O$ and nicotinic acid. Yield: 22% (based on dysprosium). Anal. Calcd for $C_{12}H_{16}ClDyN_2O_8$: C, 28.00; H, 3.11; N, 5.45. Found: C, 27.27; H, 3.04; N, 5.32. Fourier transform IR (KBr, cm^{-1}): 3429(vs), 3254(vs), 3036(w), 2813(s), 2362(w), 2230(m), 1963(w), 1591(vs), 1549(vs), 1501(vs), 1410(vs), 1230(s), 1060(s), 1010(vs), 853(s), 773(s), 715(m) and 684(m).

X-ray Crystallographic Studies. The intensity data sets were collected on Rigaku AFC-8 X-ray diffractometers with graphite monochromated Mo-Kα radiation ($\lambda = 0.71073$ Å) using an ω scan technique. CrystalClear software was used for data reduction and empirical absorption corrections.[42,43a] The structures were solved by the direct methods using the Siemens SHELXTL Version 5 package of crystallographic software.[43b] The difference Fourier maps based on these atomic positions yield the other non-hydrogen atoms. The hydrogen atom positions were generated symmetrically, allowed to ride on their respective parent atoms, and included in the structure factor calculations with assigned isotropic thermal parameters. The structures were refined using a full-matrix least-squares refinement on F^2. All atoms except for hydrogen atoms were refined anisotropically.

Results and Discussion

General Characterization. The IR spectra of **1**−**6** show similar features with bands mainly located in the range of 650−1650 cm^{-1}, as shown in Supporting Information, Figure S1. The IR spectra of **1**−**6** are obviously different from those of free nicotinic/isonicotinic acid ligands, indicating that the nicotinic/isonicotinic acids are coordinated to a metal. The broad and intense vibrations in the range of 3100−3500 cm^{-1} are assigned to the characteristic peaks of OH vibration of water molecules. The intense vibrations located at around 1590 cm^{-1} and 1410 cm^{-1} correspond to the asymmetric and symmetric stretching vibrations of the carboxylate group of

(42) (a) Rigaku *CrystalClear*, Version 1.3.5; Rigaku Corporation: The Woodlands, TX, 2002. (b) Rigaku *CrystalStructure*, Version 3.6.0; Rigaku Corporation: The Woodlands, TX, 2002.
(43) (a) Siemens *SAINT Software Reference Manual*; Siemens Energy & Automation Inc.: Madison, WI, 1994. (b) Siemens *SHELXTL, Reference Manual*, Version 5; Siemens Energy & Automation Inc.: Madison, WI, 1994.

Table 1. Crystal Parameters of Complexes **1**−**6**

complexes	**1**	**2**	**3**	**4**	**5**	**6**
formula	$C_{36}H_{32}N_6O_{16}Tb_2$	$C_{36}H_{32}Er_2N_6O_{16}$	$C_{12}H_{16}ClN_2O_8Sm$	$C_{12}H_{16}ClEuN_2O_8$	$C_{12}H_{16}ClN_2O_8Tb$	$C_{12}H_{16}ClDyN_2O_8$
Fw	1122.54	1139.20	502.07	503.68	510.64	514.22
color	colorless	pink	yellow	yellow	colorless	colorless
crystal size/mm^3	0.20 0.12 0.10	0.21 0.15 0.15	0.25 0.15 0.07	0.22 0.11 0.08	0.40 0.12 0.10	0.25 0.12 0.10
crystal system	monoclinic	monoclinic	orthorhombic	orthorhombic	orthorhombic	orthorhombic
space group	$P2_1/c$	$P2_1/c$	*Pbcn*	*Pbcn*	*Pbcn*	*Pbcn*
a (Å)	9.579(1)	9.525(1)	8.892(2)	8.882(2)	8.869(2)	8.854(4)
b (Å)	11.562(2)	11.478(1)	19.643(5)	19.625(4)	19.589(4)	19.535(9)
c (Å)	17.705(2)	17.783(2)	10.076(2)	10.048(2)	10.001(2)	9.946(4)
β (deg)	92.398(2)	91.93				
V (Å^3)	1959.2(4)	1943.1(4)	1760.0(7)	1751.4(7)	1737.4(6)	1721(1)
Z	2	2	4	4	4	4
$2\theta_{max}$ (deg)	50	50	50	50	50	50
reflections collected	12434	12267	10608	10479	10440	9783
independent, observed reflections (R_{int})	3412, 3269 (0.0249)	3427, 3298 (0.0206)	1550, 1442 (0.0298)	1544, 1404 (0.0452)	1535, 1463 (0.0246)	1399, 1300 (0.0417)
$d_{calcd.}$ (g/cm^3)	1.903	1.947	1.895	1.910	1.952	1.985
μ(mm^{-1})	3.662	4.372	3.529	3.774	4.265	4.539
T (*K*)	123.15	123.15	123.15	123.15	123.15	123.15
F(000)	1096	1108	980	984	992	996
*R*1, *wR*2	0.0177, 0.0417	0.0209, 0.0543	0.0221, 0.0519	0.0313, 0.0625	0.0217, 0.0499	0.0347, 0.0843
S	1.063	1.106	1.154	1.194	1.161	0.991
largest and mean Δ/σ	0.001, 0	0.001, 0	0, 0	0, 0	0, 0	0, 0
$\Delta\rho$(max/min) (e/Å^3)	0.968/−0.469	1.011/−0.848	0.635/−0.792	1.205/−0.639	1.163/−0.712	1.694/−0.713

the nicotinic/isonicotinic acid ligands, respectively. The absence of intense bands at about 1690−1730 cm^{-1} indicates that the nicotinic/isonicotinic acids are deprotonated.

Crystal Structures. $Ln_2(H_2O)_4(C_6NO_2H_4)_6$ (Ln = Tb (1) and Er (2)). The summary of crystallographic data and structure analyses is listed in Table 1. Selected bond lengths and bond angles are presented in Supporting Information, Table S1.

X-ray diffraction analysis reveals that complexes **1** and **2** are isomorphous, and herein only complex **1** is discussed in detail. An Oak Ridge Thermal Ellipsoid Plot (ORTEP) drawing of **1** is shown in Figure 1. Single-crystal X-ray diffraction analysis revealed that **1** consists of neutral homodinuclear $Tb_2(H_2O)_4(C_6NO_2H_4)_6$ molecules and crystallizes in the space group $P2_1/c$. Each Tb^{3+} ion is an eight-coordination, being bound by eight oxygen atoms of which two come from a chelating nicotinic acid ligand, four from four bridging nicotinic acid ligands, and two from two water molecules. The coordination sphere of Tb^{3+} ion can be described as a distorted square antiprism with the top and bottom planes defined by O(1W), O(2W), O(5), O(6) and O(1), O(3), O(2)(−2 − *x*, 1 − *y*, −1 − *z*), O(4)(−2 − *x*, 1 − *y*, −1 − *z*) atoms, respectively. The bond lengths of Tb−O range from 2.321(2) to 2.521(2) Å with an average value of 2.392(2) Å, which is comparable to that found in the literature.[44−46] Bond valence calculations indicate that the terbium ion is in a +3 oxidation state [Tb(1): 3.21].[47,48] In **1**, there are three crystallographically independent nicotinato ligands that are divided into two kinds, that is, chelating and bridging (Figure 1 and Scheme 1c and d). The bond lengths of $Tb-O_{chelating\ nicotinato}$ (mean value = 2.490(2) Å) are obviously longer than those of $Tb-O_{bridging\ nicotinato}$ (average value = 2.342(2) Å). No π-π stacking interactions are recognized between the adjacent nicotinic acid ligands in **1**. Two terbium ions are interconnected via four bridging nicotinato ligands to give a lantern-like dimer. The distance between the two terbium ions in the dimeric unit is 4.3401(5) Å, being comparable with the Tb···Tb separations documented in the literature.[44,49,50] The dimers are mutually bridged through the O1W···N1(−1 + *x*, *y*, *z*) [2.737(3) Å] hydrogen bonds to form a chain running along the [1, 0, 0] direction. The chains are linked to each other via the O2W···N3(*x*, 1/2 − *y*, −1/2 + *z*) [2.722(3) Å] hydrogen bonds to yield a slab extending along the *bc* plane, and the slabs are further interconnected together by the O1W···N2(−*x*, −1/2 + *y*, 1/2 − *z*) [2.849(3) Å] hydrogen bonds, constructing a three-dimensional (3-D) supramolecular hydrogen-bonding network (Figure 2).

$[Ln(H_2O)_4(C_6NO_2H_4)_2]_n \cdot nCl$ (Ln = Sm (3), Eu (4), Tb (5), and Dy (6)). Complexes **3**−**6** are isostructural and complex **5** is presented as an example here. X-ray diffraction analysis reveals that the structure of **5** consists of 1-D $[Tb(H_2O)_4(C_6NO_2H_4)_2]_n^{n+}$ polycationic chains and isolated chloride anions, as shown in Figures 3 and 4. Complex **5** crystallizes in the space group *Pbcn* of the orthorhombic system with four formula units in a cell. All crystallographically independent atoms are in general positions except for the Tb1 and Cl1 atoms, and the occupancies of the Tb1 and Cl1 atoms are set to 0.5 to get rational structure model and thermal displacement parameters. The terbium atom is coordinated by eight oxygen atoms, of which four are from four water molecules and others are from four isonicotinic acid ligands, yielding a slightly distorted square antiprism with the top and bottom planes defined by O(1W)(−*x*, *y*, 2.5 − *z*), O(2)(−*x*, −*y*, 2 − *z*), O(2W)(−*x*, *y*, 2.5 − *z*), O(1)

(44) Brzyska, W.; Rzaczynska, Z.; Swita, E.; Mrozek, R.; Glowiak, T. *J. Coord. Chem.* **1997**, *41*, 1.
(45) Duan, Z.; Hu, N.; Jin, Z.; Ni, J. *Chinese J. Struct. Chem* **1988**, *7*, 115.
(46) Jones, C.; Junk, P. C.; Smith, M. K.; Thomas, R. C. *Z. Anorg. Allg. Chem.* **2000**, *626*, 2491.
(47) Brown, I. D.; Altermat, D. *Acta Crystallogr. B.* **1985**, *41*, 244.
(48) O'Keeffe, M.; Brese, N. E. *J. Am. Chem. Soc.* **1991**, *113*, 3226.
(49) Crisci, G.; Meyer, G. *Z. Anorg. Allg. Chem.* **1998**, *624*, 927.
(50) Ma, J.-F.; Jin, Z.-S.; Ni, J.-Z. *Acta Crystallogr., Sect. C* **1994**, *50*, 1008.

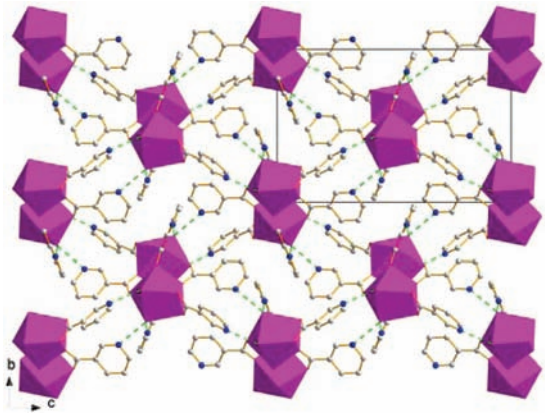

Figure 2. Packing diagram of **1** with the dashed lines representing hydrogen bonds (Å): O1W···N1($-1+x$, y, z) 2.737(3), O1W···N2($-x$, $-1/2+y$, $1/2-z$) 2.849(3), and O2W···N3(x, $1/2-y$, $-1/2+z$) 2.722(3).

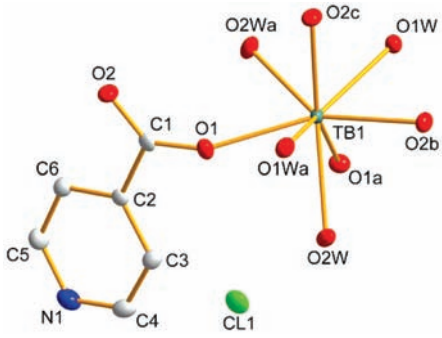

Figure 3. ORTEP drawing of **5** with 50% thermal ellipsoids. Hydrogen atoms were omitted for clarity. Symmetry codes: a. $-x$, y, $2.5-z$; b. x, $-y$, $0.5+z$; c. $-x$, $-y$, $2-z$.

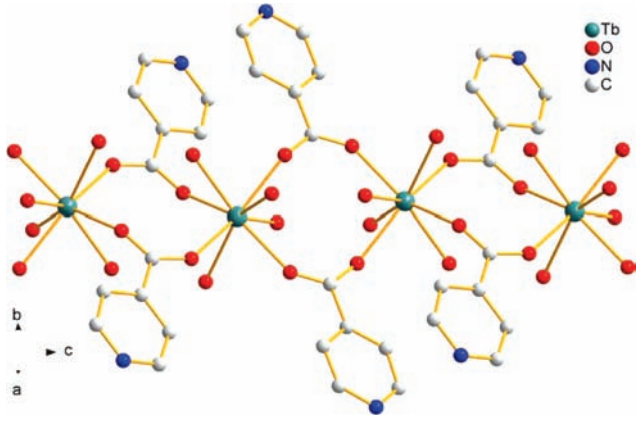

Figure 4. 1-D chain-like structure of **5**.

and O(1W), O(2)(x, $-y$, $0.5+z$), O(2W), O(1)($-x$, y, $2.5-z$) atoms, respectively. The isonicotinic acid ligands act as bidentate ligands to bridge the terbium ions (Scheme 1 (d′)). The bond lengths of Tb−$O_{isonicotinato}$ range from 2.311(2) to 2.334(2) Å with an average value of 2.322(2) Å, which is obviously shorter than that of Tb−O_{water} being of 2.425(2) and 2.478(2) Å, suggesting that isonicotinic acid ligand has a stronger affinity to Tb^{III} ion than that of water. The mean Ln−O bond lengths in **3**−**6** accord to the order of Sm−O [2.426(2) Å] > Eu−O [2.413(3) Å] > Tb−O [2.387(2) Å] > Dy−O [2.371(2) Å], which is due to the effect of the lanthanide contraction. The result of the bond valence calculations show that the terbium ion has a +3 oxidation state [Tb(1): 3.26]. Since the oxidation states of the chloride anion and the terbium cation are −1 and +3, respectively, each isonicotinic acid ligand should be in a −1 oxidation state to keep the charge balance of complex **5**, as is the case found in other isonicotinic acid-containing complexes.[51,52] The neighboring terbium ions are bridged via two μ_2-isonicotinic acid ligands in a 2−2−2 fashion (the number indicates the number of the bridging ligands) to construct a 1-D polycationic chain running along the c direction with the Tb···Tb distance being of 5.020(1) Å, which is significantly longer than the Tb···Tb separation [4.3401(5) Å] in the dimeric unit of complex **1** (Figure 4). This discrepancy is probably due to the different amounts of bridging ligands between two metal ions: more bridging ligands may, in effect, weaken the repulsion between two metal cations and draw them closer.

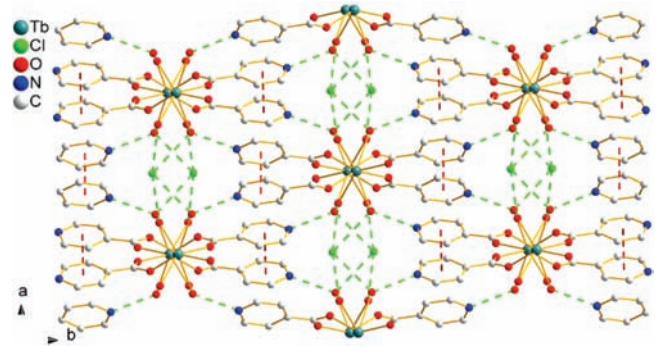

Figure 5. Packing diagram of **5** with the red dashed lines representing π-π stacking interactions and the green dashed lines representing hydrogen bonds (Å′): O1W···Cl1($1+x$, y, z) 3.197(2), O1W···O2W($-x$, $-y$, $3-z$) 2.847(3), O1W···N1($0.5+x$, $0.5+y$, $2.5-z$) 2.700(4), and O2W···Cl1 3.030(2).

There are three kinds of hydrogen bonds in **5**, that is, O···Cl, O···O, and O···N hydrogen bonds, including O1W···Cl1($1+x$, y, z), O2W···Cl1, O1W···O2W($-x$, $-y$, $3-z$), and O1W···N1($0.5+x$, $0.5+y$, $2.5-z$) with the hydrogen bond distances being of 3.197(2), 3.030(2), 2.847(3), and 2.700(4) Å, respectively. In **5**, some π-π stacking interactions exist between two adjacent isonicotinic acid ligands located in a same chain. For clarity, we define the pyridyl ring of the isonicotinic acid ligand as R1. The R1 ring in an isonicotinic acid ligand has a π-π contact with a R1′ ring in an adjacent isonicotinic acid ligand. The centroid to centroid distance is 3.766(2) Å for rings R1 and R1′. The perpendicular separation between R1 and R1′ is about 3.423 Å. R1 slides from R1′ by about 1.570 Å. The dihedral angle is 1.37° between R1 and R1′. The 1-D polycationic $[Tb(H_2O)_4(C_6NO_2H_4)_2]_n^{n+}$ chains and the isolated chloride anions are linked via hydrogen bonds and π-π stacking interactions to complete a 3-D supramolecular network, as shown in Figure 5.

Properties. UV−vis Absorption Spectroscopy. Figure 6a displays the UV−vis absorption spectra for nicotinic acid and its lanthanide (Tb and Er) complexes (**1** and **2**). Both

(51) Ma, L.; Evans, O. R.; Foxman, B. M.; Lin, W. *Inorg. Chem.* **1999**, *38*, 5837.
(52) Zeng, X.-R.; Xu, Y.; Xiong, R.-G.; Zhang, L.-J.; You, X.-Z. *Acta Crystallogr., Sect. C* **2000**, *56*, e325.

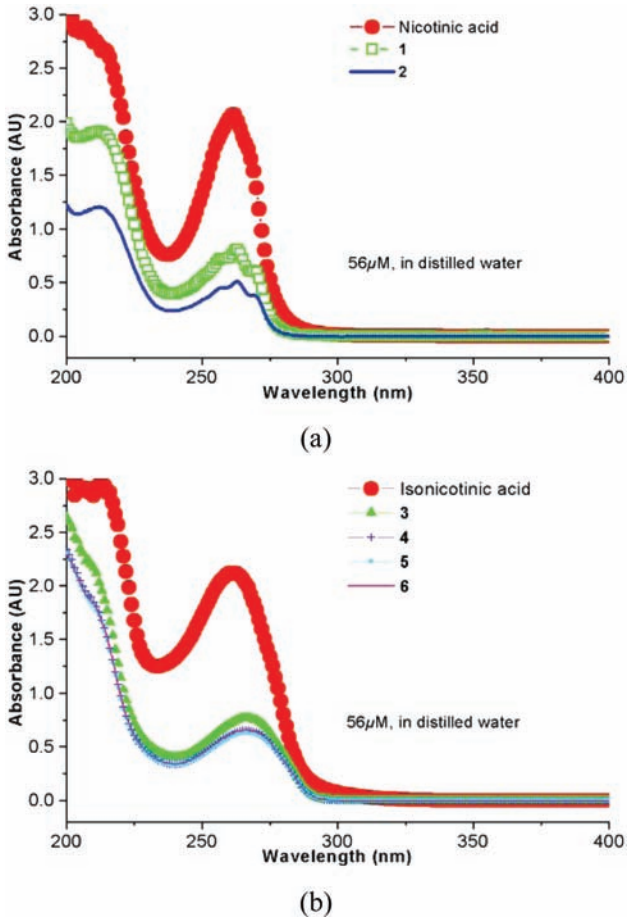

Figure 6. UV−vis absorption spectra measured in distilled water (56 μM) at room temperature: (a) **1**, **2**, and nicotinic acid (red, nicotinic acid; green, **1**; blue, **2**); (b) **3**−**6** and isonicotinic acid (red, isonicotinic acid; green, **3**; blue, **4**; cyan, **5**; violet, **6**). Molar absorption coefficients (ε/$M^{-1}cm^{-1}$): $\varepsilon_{212\ nm}$ = 34108 (**1**) and 21429 (**2**), $\varepsilon_{263\ nm}$ = 14553 (**1**) and 9178 (**2**), $\varepsilon_{261\ nm}$ = 36965 (nicotinic acid), $\varepsilon_{262\ nm}$ = 37858 (isonicotinic acid), and $\varepsilon_{266\ nm}$ = 13786 (**3**), 11696 (**4**), 11392 (**5**), and 11750 (**6**).

complexes **1** and **2** have two absorption bands located at 212 (ε = 34108 and 21429 $M^{-1}cm^{-1}$ for **1** and **2**, respectively) and 263 nm (ε = 14553 and 9178 $M^{-1}cm^{-1}$ for **1** and **2**, respectively), while nicotinic acid only exhibits one absorption band at 261 nm (ε = 36965 $M^{-1}cm^{-1}$). For complexes **1** and **2**, the absorption band at 263 nm is slightly red-shifted as compared to that of nicotinic acid, suggesting that the coordination interaction between the lanthanide ions and the nicotinic acid yields a more extensive $\pi\rightarrow\pi^*$ conjugated system than free nicotinic acid ligand. The absorption intensity of nicotinic acid is far stronger than that of **1** and **2**, and complex **2** has the weakest absorption among them.

Figure 6b gives the UV−vis absorption spectra for isonicotinic acid and complexes **3**−**6**. Isonicotinic acid has a strong absorption at 262 nm (ε = 37858 $M^{-1}cm^{-1}$), while complexes **3**−**6** show a main absorption band at 266 nm (ε = 13786, 11696, 11392, and 11750 $M^{-1}cm^{-1}$ for **3**−**6**, respectively), which is red-shifted by 4 nm compared with isonicotinic acid. This is characteristic absorption of isonicotinic acid. Similar to the case between nicotinic acid and complexes **1** and **2**, the absorption intensity of isonicotinic acid is at least twice stronger than that of **3**−**6**, clearly

Table 2. Energy Difference between the Lowest Triplet Energy of Isonicotinic/Nicotinic Acid and the Resonant Energy Level of the Ln^{3+} Ion (Sm^{3+}($^4G_{5/2}$, 17900 cm^{-1}), Eu^{3+}($^5D_1$, 18674 cm^{-1}), Tb^{3+}($^5D_4$, 20500 cm^{-1}), and Dy^{3+}($^4F_{9/2}$, 20875 cm^{-1}))

	lowest triplet state energy (Tr) (cm^{-1})		ΔE(Tr-Ln^{3+}) (cm^{-1})	
Ln^{3+}	isonicotinic acid	nicotinic acid	isonicotinic acid	nicotinic acid
Sm	23041	23923	5141	
Eu	23041	23923	4367	
Tb	23041	23923	2541	3423
Dy	23041	23923	2166	

implying that the coordination to metal ions will decrease the absorption intensity of isonicotinic/nicotinic acid ligand. The obvious difference in the UV−vis absorption spectra between **1**−**2** and **3**−**6** may be caused by the fact that, compared to the dimeric complexes **1** and **2**, the 1-D chain-like complexes **3**−**6** have a more extended structure that allows them to form a more extensive $\pi\rightarrow\pi^*$ conjugated system and, as a result, complexes **3**−**6** display a larger red-shift than **1** and **2**.

Photoluminescence. The low temperature (77 K) phosphorescence spectra of nicotinic acid and isonicotinic acid ligands were measured and shown in the Supporting Information, Figure S2. From the estimation of the onset of the emission bands (418 nm for nicotinic acid and 434 nm for isonicotinic acid, respectively), the lowest triplet state energies can be determined as 23923 cm^{-1} and 23041 cm^{-1} for nicotinic acid and isonicotinic acid, respectively.[24,53,54] The energy differences between the lowest triplet state of nicotinic/isonicotinic acid and the resonant energy levels of Sm^{3+}($^4G_{5/2}$, 17900 cm^{-1}), Eu^{3+} ($^5D_1$, 18674 cm^{-1}), Tb^{3+} ($^5D_4$, 20500 cm^{-1}), and Dy^{3+} ($^4F_{9/2}$, 20875 cm^{-1}) can be calculated and the results are listed in Table 2.

According to the intramolecular energy transfer mechanism reported by Dexter and Sato et al.,[55−59] the intramolecular energy migration efficiency depends mainly on two energy transfer processes, namely, (a) the energy transfer from the lowest triplet energy level of the ligand to the resonant energy level of the lanthanide ion by Dexter's resonant exchange interaction; and (b) the inverse energy transfer from Ln^{3+} ion to organic ligand by a thermal deactivation mechanism. If the energy difference is too small, the inverse energy transfer will take place much easier. Both energy transfer processes depend on the energy gap between the lowest triplet energy level of the organic ligand and the resonant energy level of the lanthanide ion. Clearly, there is an opposite influence between two energy transfer processes. On the basis of the intramolecular energy transfer mechanism, an optimal value of the energy gap is assumed to exist around 3000 ± 500 cm^{-1}.[60] The larger or the smaller energy difference may result in a decrease in the photoluminescent

(53) Archer, R. D.; Chen, H. *Inorg. Chem.* **1998**, *37*, 2089.
(54) Sato, S.; Wada, M. *Bull. Chem. Soc. Jpn.* **1970**, *43*, 1955.
(55) Dexter, D. L. *J. Chem. Phys.* **1953**, *21*, 836.
(56) Wu, S. L.; Wu, Y. L.; Yang, Y. S. *J. Alloys Compd.* **1994**, *180*, 399.
(57) Yan, B.; Zhang, H. J.; Wang, S. B.; Ni, J. Z. *Monafsh. Chem.* **1998**, *129*, 151.
(58) Brown, T. D.; Shepherd, T. M. *J. Chem. Soc., Dalton Trans.* **1973**, 336.
(59) Kleinerman, M. *J. Chem. Phys.* **1969**, *51* (6), 2370.
(60) Xu, B.; Yan, B. *Spectrochim. Acta A* **2007**, *66*, 236.

Scheme 2. Schematic and Partial Energy Level Diagram of the Main Energy Absorption, Transfer, and Luminescence Processes in **1**−**6** and the Nicotinic/Isonicotinic Acid Ligands

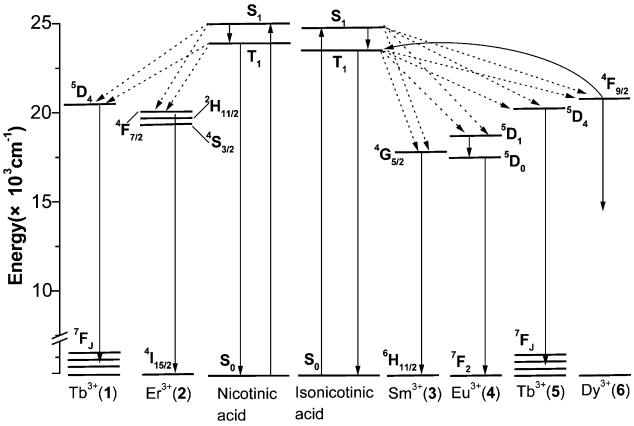

intensities of the lanthanide-containing complexes. However, the estimated optimal value may not be accurate because some factors, such as the oscillation of coordinated water molecules, that can also affect photoluminescent properties are not included into the estimation.

As shown in Table 2, the energy difference for Eu^{3+} is too large (4367 cm^{-1}), indicating that isonicotinic acid is probably not suitable for the excitation of Eu^{3+} ion. The energy difference for Sm^{3+} is also large (5141 cm^{-1}), and, moreover, the numerous internal energy levels existing between the first excited singlet state and the ground-state of the Sm^{3+} ions can easily cause nonradiative energy transfer, losing the excitation energy of the isonicotinic acid. As a result, it can be predicted that Sm^{3+}-containing complex **3** would not exhibit excellent photoluminescence. Comparing with that of Eu^{3+} and Sm^{3+} ions, the energy difference of Tb^{3+} ion is much smaller. This implies that nicotinic acid and isonicotinic acid are more suitable for the photoluminescence of Tb^{3+} than Sm^{3+} and Eu^{3+}. Oppositely, Dy^{3+}-containing complex **6** has the smallest energy difference among the title complexes, 2166 cm^{-1}, and is small enough to assume a more competitive inverse energy transfer when compared with **1**−**5**. Such a small energy difference would allow increased inverse energy transfer from the resonant emissive energy level of $^4F_{9/2}$ of Dy^{3+} to the lowest triplet state of isonicotinic acid ligand (Scheme 2). Therefore, it can be expected that complex **6** may not display good photoluminescent properties.

Taking into account the excellent photoluminescent properties of Tb^{3+} ion, the photoluminescent spectra of **1** and **5** were investigated at room temperature (Figure 7). As shown in Figure 7, the emission spectra of **1** and **5** are very similar, and both of them exhibit good photoluminescent properties with narrow, sharp, and well-separated bands. This is in good agreement with the fact that their energy differences (3423 and 2541 cm^{-1}, respectively) are close to the optimal value of the energy gap (3000 ± 500 cm^{-1}). The solid-state excitation spectra of **1** and **5** show that the effective energy absorption mainly takes place in the ultraviolet region of the range 300−390 nm. The excitation bands of **1** under the green emission of 548 nm possess three main peaks, 340, 370, and 378 nm, respectively. Similarly, under the green

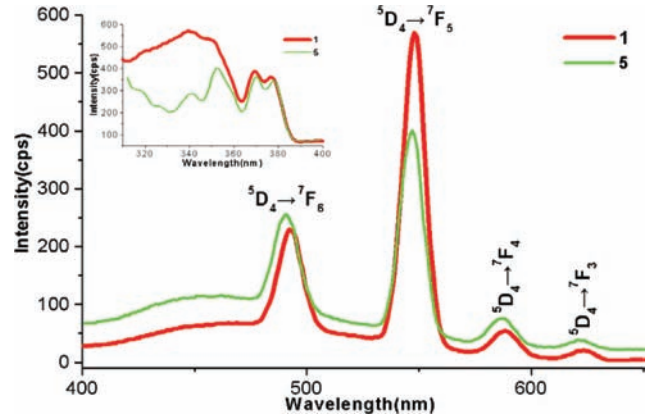

Figure 7. Solid-state emission (outer) and excitation (inner) spectra of **1** (red) and **5** (green) at room temperature.

emission of 545 nm the excitation bands of **5** show four main peaks, 341, 351, 370, and 379 nm, respectively. The sharp features at around 370 nm for both complexes correspond most probably to an f-f transition of Tb (4f-3d transition should occur around 320−330 nm). For complexes **2**−**4** and **6**, a sharp band at around 370 nm can also be found in their excitation spectra, which is likewise ascribed to f-f transition of lanthanide ions (Supporting Information, Figures S3−S6). We further measured the corresponding emission spectra of **1** and **5** by selective excitation with different excitation wavelengths, and they show similar emission positions except for slight difference in the photoluminescent intensities. This suggests that all of the excitation bands are effective for the photoluminescence of Tb^{3+} ion in **1** and **5**. For complex **1**, the emission spectra show four emission bands upon excitation at 340 nm: 492, 548, 588, and 623 nm, corresponding to the characteristic emission $^5D_4-^7F_J$ transitions (J = 6, 5, 4, and 3, respectively) of Tb^{3+} ions (Figure 7).[26,61,62] This indicates that effective energy transfer occurs and that conjugated systems are formed between the ligands and the chelated lanthanide ions in **1**. Among the four characteristic emission $^5D_4-^7F_J$ transitions (J = 6, 5, 4, and 3) of Tb^{3+} ions, the intensity of the green luminescent of $^5D_4-^7F_5$ transition is the strongest. As for complex **5**, under the excitation of 351 nm the emission spectra also display four emission bands: 491, 545, 586, and 622 nm, which correspond to the $^5D_4-^7F_J$ transitions (J = 6, 5, 4, and 3, respectively) of the Tb^{3+} ion (Figure 7).

The quantum yield of the solid-state sample of **5** is determined to be 21%. The solid-state sample of complex **1** displays a much higher quantum yield of around 44%, which is higher than that of many terbium-containing complexes,[63−74] even though lower than that of some others.[75−79]

(61) Viswanathan, S.; Bettencourt-Dias, A. *Inorg. Chem. Commun.* **2006**, *9*, 444.
(62) Horiuchi, T.; Iki, N.; Hoshino, H.; Kabutob, C.; Miyano, S. *Tetrahedron Lett.* **2007**, *48*, 821.
(63) Daiguebonne, C.; Kerbellec, N.; Guillou, O.; Bünzli, J. C.; Gumy, F.; Catala, L.; Mallah, T.; Audebrand, N.; Gérault, Y.; Bernot, K.; Calvez, G. *Inorg. Chem.* **2008**, *47* (9), 3700.
(64) Picard, C.; Geum, N.; Nasso, I.; Mestre, B.; Tisnès, P.; Laurent, S.; Muller, R. N.; Elst, L. V. *Bioorg. Med. Chem. Lett.* **2006**, *16*, 5309.
(65) Hnatejko, Z.; Elbanowski, M. *J. Alloys Compd.* **2004**, *380*, 181.
(66) Brunet, E.; Juanes, O.; Rodríguez-Blasco, M. A.; Vila-Nueva, S. P.; Garayalde, D.; Rodríguez-Ubis, J. C. *Tetrahedron Lett.* **2005**, *46*, 7801.

Therefore, complex **1** has better photoluminescence performance than complex **5**. The discrepancy of the quantum yields between **1** and **5** may be ascribed to their different structural motifs. The Tb^{3+} ion in **1** coordinates to five nicotinic acid ligands and two water molecules, while it binds to four isonicotinic acid ligands and four water molecules in **5**. Thus, the Tb^{3+} ion in **1** has more "antenna" ligands that can absorb more light energy, which result in a higher quantum yield as compared to complex **5**. In addition, coordination of water molecules would generally decrease the photoluminescence intensity of a lanthanide complex because the thermal oscillation of the water molecules consumes some excitation energy absorbed by "antenna" ligands. The Tb^{3+} ion in **1** has less coordination water molecules than that in **5**, which leads to less deactivation in **1**. Therefore, it is reasoned that more "antenna" ligands and less deactivation make complex **1** exhibit a higher quantum yield than complex **5**.

The solid-state photoluminescence spectra of **2**−**4** and **6** were also investigated at room temperature (Supporting Information, Figures S3−S6). The predominant ligand-based emission is probably caused by the fact that the lowest triplet state energy level of the ligand does not match well to the resonance level of the Ln^{3+} ions. However, the existence (even though it is small in intensity) of the characteristic emission bands of the Ln^{3+} ions for **2**−**4** suggests that the intramolecular energy transfer process still exists between the ligand and the Ln^{3+} ion. In **6**, the absence of the emission of Dy^{3+} ions may be attributed to the small energy difference (2166 cm^{-1}) between the lowest triplet energy level of the ligand and the resonant emissive energy level of Dy^{3+} ions. Such a small energy difference may allow increased inverse energy transfer from the resonant emissive energy level of the Dy^{3+} ion to the lowest triplet state of the ligand and, as a result, no characteristic emission bands of Dy^{3+} ions can be observed.

Conclusion

In conclusion, by using an ultrasonic synthesis method, two series of six lanthanide complexes with nicotinic/isonicotinic acid as ligands have been synthesized and characterized. X-ray structural analysis reveals that they are grouped into two structural motifs, that is, dimeric and 1-D chain-like polymeric structures. The photophysical properties of the title complexes and their ligands have been studied with UV−vis absorption spectra, low temperature phosphorescence spectra, quantum yield, excitation and emission spectra. The energy match between nicotinic/isonicotinic acid ligands and lanthanide ions in **1**−**6** has been studied to predict the energy transfer existing between the ligands and the Ln^{3+} ions. The results of photoluminescence research on the title complexes are in good agreement with the prediction from the energy match and intramolecular energy transfer. On the basis of the investigation of the relationship between the crystal structures and the photoluminescent properties, it is believed that many factors can affect photoluminescent properties, such as the types of metal centers and organic ligands, the extent of the conjugation of the complex, the number of the coordinated water molecules, the number of the "antenna", and so forth. Future research in our laboratory will explore other lanthanide systems to gain more insight into the relationship between the crystal structures and the photoluminescent properties. This will eventually allow us to "logically" prepare novel photoluminescent materials with the desired properties for potential applications.

Acknowledgment. This work was supported by a Grant-in-Aid (No. 19205019), and a Global COE program, "the Global Education and Research Center for Bio-Environmental Chemistry" from the Ministry of Education, Culture, Sports, Science and Technology.

Supporting Information Available: X-ray crystallographic files in CIF format for **1**−**6**, IR spectra, phosphorescence spectra of nicotinic acid and isonicotinic acid, and solid-state emission spectra of complexes **2**, **3**, **4**, and **6**. This material is available free of charge via the Internet at http://pubs.acs.org.

IC9000279

(67) Chatterton, N.; Bretonnière, Y.; Pécaut, J.; Mazzanti, M. *Angew. Chem., Int. Ed.* **2005**, *44*, 7595.
(68) Gawryszewska, P.; Sokolnicki, J.; Dossing, A.; Riehl, J. P.; Muller, G.; Legendziewicz, J. *J. Phys. Chem. A* **2005**, *109*, 3858.
(69) De Silva, C. R.; Li, J.; Zheng, Z.; Corrales, L. R. *J. Phys. Chem. A* **2008**, *112*, 4527.
(70) Tedeschi, C.; Azéma, J.; Gornitzka, H.; Tisnès, P.; Picard, C. *Dalton Trans.* **2003**, 1738.
(71) Tan, M.; Song, B.; Wang, G.; Yuan, J. *Free Radical Biol. Med.* **2006**, *40*, 1644.
(72) de Bettencourt-Dias, A.; Viswanathan, S. *Chem. Commun.* **2004**, 1024.
(73) Reshmi, J. R.; Biju, S.; Reddy, M. L. P. *Inorg. Chem. Commun.* **2007**, *10*, 1091.
(74) Charbonnière, L. J.; Balsiger, C.; Schenk, K. J.; Bünzli, J.-C. G. *J. Chem. Soc., Dalton Trans.* **1998**, 505.
(75) Bredol, M.; Kynast, U.; Ronda, C. *Adv. Mater.* **1991**, *3*, 361.
(76) Brunet, E.; Juanes, O.; Sedano, R.; Rodríguez-Ubis, J. C. *Photochem. Photobiol. Sci.* **2002**, *1*, 613.
(77) Kang, J.-G.; Kim, T.-J.; Kang, H.-J.; Kang, S. K. *J. Photochem. Photobiol. A* **2005**, *174*, 28.
(78) Lill, D. T.; de Bettencourt-Dias, A.; Cahill, C. L. *Inorg. Chem.* **2007**, *46*, 3960.
(79) Natrajan, L. S.; Timmins, P. L.; Lunn, M.; Heath, S. L. *Inorg. Chem.* **2007**, *46*, 10877.